

Experimental Investigation and *R*-matrix Analysis of Low-lying Levels in ${}^5\text{He}$ and ${}^5\text{Li}$

C. L. Woods, F. C. Barker,^A W. N. Catford, L. K. Fifield and N. A. Orr

Department of Nuclear Physics, Research School of Physical Sciences,
Australian National University, G.P.O. Box 4, Canberra, A.C.T. 2601, Australia.

^A Department of Theoretical Physics, Research School of Physical Sciences,
Australian National University, G.P.O. Box 4, Canberra, A.C.T. 2601, Australia.

Abstract

The particle-unstable nuclei ${}^5\text{He}$ and ${}^5\text{Li}$ have been studied via the ${}^4\text{He}({}^7\text{Li}, {}^6\text{Li}){}^5\text{He}$ and ${}^4\text{He}({}^7\text{Li}, {}^6\text{He}){}^5\text{Li}$ stripping reactions at beam energies of 50 MeV and the ${}^6\text{Li}({}^{12}\text{C}, {}^{13}\text{N}){}^5\text{He}$ and ${}^6\text{Li}({}^{13}\text{C}, {}^{14}\text{C}){}^5\text{Li}$ pickup reactions at 90 MeV. The experimental data clearly demonstrate a dependence of the lineshapes on the method of production of the mass-5 nuclei (in this case pickup or stripping). The observed lineshapes were analysed using the *R*-matrix formalism in a two-level approximation for each J^π value, with parameter values deduced from fits to the available ${}^4\text{He} + \text{nucleon}$ scattering data. A best channel radius of 5.5 ± 1.0 fm was determined from the stripping data, and the corresponding set of *R*-matrix parameters also provided a satisfactory description of the pickup data. This channel radius is significantly larger than that employed in most previous analyses. Properties of the lowest $\frac{3}{2}^-$ and $\frac{1}{2}^-$ states of ${}^5\text{He}$ and ${}^5\text{Li}$, observed via direct reactions, are deduced from the parameter values. These properties are compared with results from earlier experimental analyses and the inferred properties of positive-parity states are compared with the results of recent shell-model calculations.

1. Introduction

This work was undertaken to obtain precise data for the nuclei ${}^5\text{He}$ and ${}^5\text{Li}$ observed via stripping and pickup reactions in order to complement existing low-energy ${}^4\text{He} + \text{nucleon}$ scattering data, and to seek a consistent *R*-matrix description of both data sets using a single set of *R*-matrix parameters.

The unbound $\frac{3}{2}^-$ ground states and $\frac{1}{2}^-$ first-excited states of ${}^5\text{He}$ and ${}^5\text{Li}$ have previously been observed both as resonances in ${}^4\text{He} + \text{nucleon}$ scattering and as particle-unstable products in a variety of reactions. The values of their energies and widths derived from the reaction data, however, show considerable scatter. This can be attributed not only to experimental difficulties and inadequate methods of analysis, but also to the different definitions used for the energy and width of an unbound state.

In a recent paper, Barker and Woods (1985, henceforth referred to as BW) performed *R*-matrix fits to each of the experimental $s_{1/2}$, $p_{1/2}$, $p_{3/2}$, $d_{3/2}$ and $d_{5/2}$ ${}^4\text{He} + \text{nucleon}$ phase shifts, for a range of values of the channel radius a , deriving values of the eigenenergies, reduced width amplitudes and boundary condition parameter for each value of a . These *R*-matrix parameters were then used to predict the peak energy (E_{max}) and FWHM ($\Gamma_{1/2}$) of the ${}^5\text{He}$ and ${}^5\text{Li}$ states as observed in reactions. For each J^π value, BW used a two-level approximation, with the upper level providing a background contribution; similarly in deriving the experimental

phase shifts from the ${}^4\text{He}+n$ scattering data, Bond and Firk (1977) had included a background contribution for each J^π , while Dodder *et al.* (1977) fitted the ${}^4\text{He}+p$ data with a background level for the $\frac{3}{2}^-$ and $\frac{1}{2}^-$ partial waves only.

It was found that the R -matrix predictions for E_{max} and $\Gamma_{1/2}$ of the reaction lineshapes depend on the choice of a , through its association with unique values of the other R -matrix parameters. Thus, although the ${}^4\text{He}+$ nucleon scattering data can be fitted satisfactorily for a wide range of a , the direct reaction data can be used in principle to select the best value of a and therefore a single set of R -matrix parameters. It was noted in BW, however, that the results of previous direct reaction studies were not sufficiently consistent to determine a single set of parameters.

It was also shown in BW that values of E_{max} and $\Gamma_{1/2}$ obtained for these levels when they are formed in direct reactions by addition of a nucleon to a ${}^4\text{He}$ target (stripping) could be different from those obtained by removal of a nucleon from a ${}^6\text{Li}$ target (pickup). The difference results from the plausible assumption that the relative feeding amplitudes to the high-lying background levels differ in the two cases. Earlier R -matrix analyses of reaction data employed a single-level approximation, in which there are no high-lying background levels and therefore no dependence of E_{max} and $\Gamma_{1/2}$ on the method of production of the mass-5 nucleus.

In the present work, new data are presented for direct reactions populating ${}^5\text{He}$ and ${}^5\text{Li}$ via stripping and pickup (Section 2). The results are analysed using the two-level R -matrix formulae given in BW and the dependence of the energies and widths of the observed lineshapes on the production mechanism is studied (Section 3). The stripping-reaction data are of sufficient precision to limit a (assumed to be the same for each J -value) to a narrow range and therefore provide a means of selecting a single set of R -matrix parameters. This parameter set is also used to describe the pickup-reaction data and, more generally, should be used in the prediction of the properties of the lower state of each spin and parity in the mass-5 nuclei observed in other reactions.

In Section 4 the results of earlier experimental studies of the $\frac{3}{2}^-$ ground states and $\frac{1}{2}^-$ first-excited states are discussed in the light of this work. Predictions for the $\frac{1}{2}^+$, $\frac{3}{2}^+$ and $\frac{5}{2}^+$ states cannot be tested directly because the large widths of these states render them unsuitable for study via direct reactions. A model-dependent test of their properties is, however, provided by recent shell-model calculations. The properties derived from previous phase-shift analyses of ${}^4\text{He}+$ nucleon scattering data are also discussed briefly in this section. The main results and conclusions are summarised in Section 5.

2. Experimental Method

The reactions and experimental conditions employed in this work are summarised in Table 1. Because the mass-5 nuclei are particle-unstable, there are always at least three final particles produced in such reactions. In any single event, it is not certain whether the detected particle has been produced in the first stage of the breakup, in which case it contributes to the lineshape one wishes to study, or in a later stage, so contributing to unwanted background. Thus in competition with the first reaction in Table 1, background ${}^6\text{Li}$ particles can be produced in the alternative mode of decay ${}^4\text{He}({}^7\text{Li}, {}^7\text{Li}^*){}^4\text{He}$ followed by ${}^7\text{Li}^* \rightarrow {}^6\text{Li}+n$.

In order to maximise the desired direct transitions relative to such alternative

Table 1. Experimental conditions

Reaction	Beam energy (MeV)		Grazing angle (lab)	Nominal angles (lab)	Composition and thickness of target	Calibration target
	lab	c.m.				
${}^4\text{He}({}^7\text{Li}, {}^6\text{Li}){}^5\text{He}$ and ${}^4\text{He}({}^7\text{Li}, {}^6\text{He}){}^5\text{Li}$	50	18.2	2.1°	6.0°	${}^4\text{He}$ gas $10 \mu\text{g cm}^{-2}$ ^A	CO_2 gas $10 \mu\text{g cm}^{-2}$ ^A
${}^6\text{Li}({}^{12}\text{C}, {}^{13}\text{N}){}^5\text{He}$	90	30.1	3.1°	3.5°, 4.4°	$70 \mu\text{g cm}^{-2}$ ${}^6\text{LiF}$ on $15 \mu\text{g cm}^{-2}$ C	$70 \mu\text{g cm}^{-2}$ ${}^7\text{LiF}$ on $15 \mu\text{g cm}^{-2}$ C
${}^6\text{Li}({}^{13}\text{C}, {}^{14}\text{C}){}^5\text{Li}$	90	28.5		5.0°		

^A Equivalent thickness of a solid target, calculated from gas pressure and length of gas visible at entrance to spectrometer.

Table 2. Summary of experimental data

Reaction	θ_{lab} (deg.)	$\theta_{\text{c.m.}}$ (deg.)	Extent of unobscured data above $\frac{3}{2}^-$ peak (MeV)	FWHM reso- lution (keV)	Total c.m. cross section to $\frac{3}{2}^-$ state (mb sr^{-1})	Disper- sion (keV/ch.)	r.m.s. uncertainty in calibration (keV)	Change in $\frac{3}{2}^-$ energy with α (keV fm^{-1})
${}^4\text{He}({}^7\text{Li}, {}^6\text{Li}){}^5\text{He}$	6.0	17.8	3.04	90	6	18	± 27	20
${}^4\text{He}({}^7\text{Li}, {}^6\text{He}){}^5\text{Li}$	6.0	21.1	4.05	100	0.5	24	± 28	60
${}^6\text{Li}({}^{12}\text{C}, {}^{13}\text{N}){}^5\text{He}$	3.62	12.3	5.22	190	20	23	± 25	3
	4.58	15.6	5.43	180	5	23	± 27	3
	5.12	17.4	3.82	200	3	23	± 21	3
${}^6\text{Li}({}^{13}\text{C}, {}^{14}\text{C}){}^5\text{Li}$	3.46	11.6	3.69	210	16	26	± 20	5
	4.61	15.5	3.45	210	3	26	± 18	5
	5.20	17.5	3.17	200	2	26	± 23	5

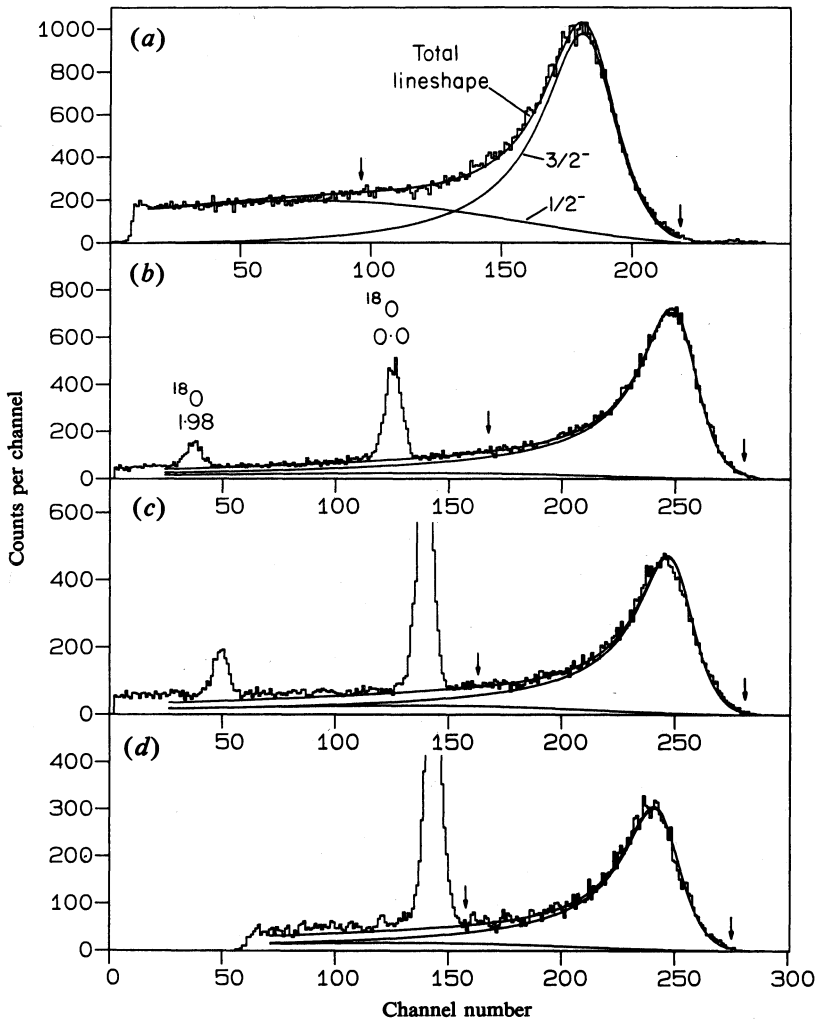


Fig. 1. Experimental data for ${}^5\text{He}$: (a) ${}^4\text{He}({}^7\text{Li}, {}^6\text{Li}){}^5\text{He}$ at 6° , (b) ${}^6\text{Li}({}^{12}\text{C}, {}^{13}\text{N}){}^5\text{He}$ at 3.62° , (c) ${}^6\text{Li}({}^{12}\text{C}, {}^{13}\text{N}){}^5\text{He}$ at 4.58° and (d) ${}^6\text{Li}({}^{12}\text{C}, {}^{13}\text{N}){}^5\text{He}$ at 5.12° , showing R -matrix fits for $\frac{3}{2}^-$, $\frac{1}{2}^-$ and total lineshapes calculated for a channel radius of $a = 5.5$ fm. Limits to the fitting regions are indicated by arrows. Peaks corresponding to reactions from target elements other than lithium are labelled by the residual nucleus and excitation energy in MeV.

decay modes, it is desirable to have a large centre-of-mass (c.m.) energy and therefore a high beam energy. Also, the direct reaction cross section peaks near the grazing angle, which is small for high c.m. energies, and therefore it is best to detect the beam-like ejectiles at forward angles. An additional consideration was that neither ${}^6\text{He}$ nor ${}^{13}\text{N}$ has any bound excited states, and the lowest in ${}^6\text{Li}$ and ${}^{14}\text{C}$ are at 3.56 and 6.09 MeV respectively, allowing observation of a substantial fraction of both the $\frac{3}{2}^-$ and $\frac{1}{2}^-$ lineshapes (Table 2).

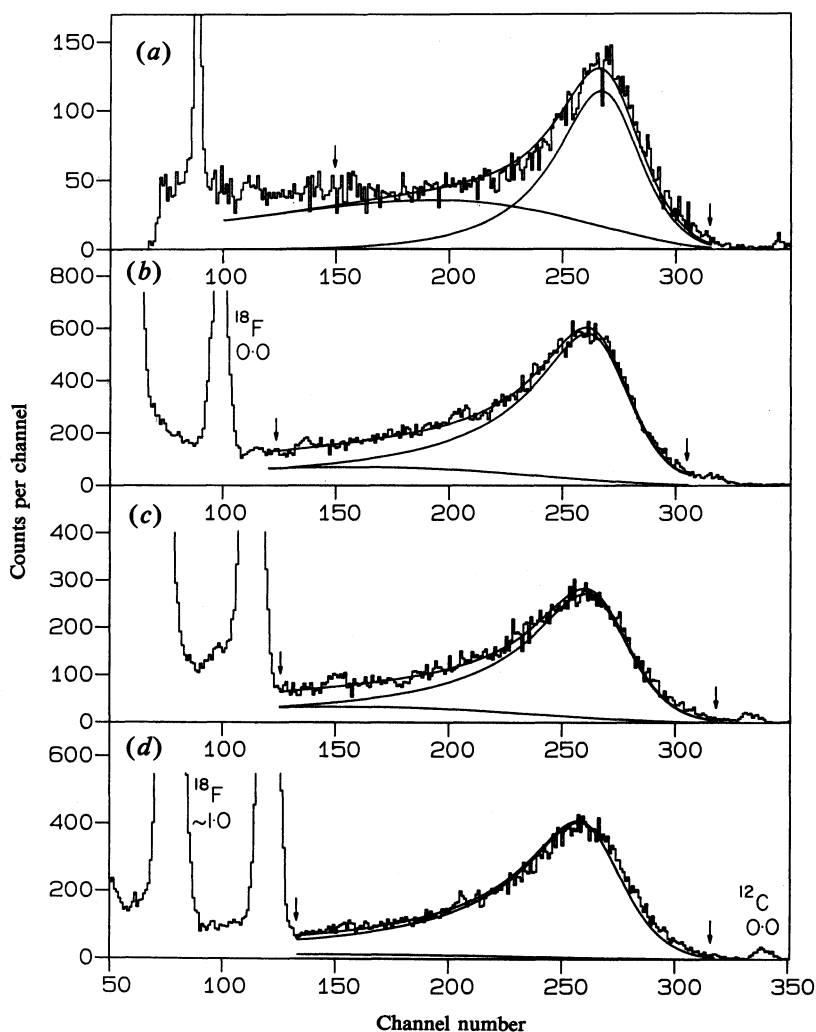


Fig. 2. Experimental data for ${}^5\text{Li}$: (a) ${}^4\text{He}({}^7\text{Li}, {}^6\text{He}){}^5\text{Li}$ at 6° , (b) ${}^6\text{Li}({}^{13}\text{C}, {}^{14}\text{C}){}^5\text{Li}$ at 3.46° , (c) ${}^6\text{Li}({}^{13}\text{C}, {}^{14}\text{C}){}^5\text{Li}$ at 4.61° and (d) ${}^6\text{Li}({}^{13}\text{C}, {}^{14}\text{C}){}^5\text{Li}$ at 5.20° . The feature at channel 88 in (a) is produced by a small fraction of elastically scattered ${}^7\text{Li}$ ions which gave degraded energy-loss signals. Other details are as in Fig. 1.

Reaction products emitted at the selected angle were momentum-analysed in an Enge split-pole spectrometer and detected in a multi-element gas-filled counter (Ophel and Johnston 1978). The spectrometer's entrance aperture subtended 0.1° in the (horizontal) reaction plane and 2.5° vertically. Because the incident ions were much heavier than the target nuclei, the momenta of the ejectiles varied rapidly with angle and the small horizontal acceptance was chosen to avoid any distortion of the mass-5 lineshapes due to imperfect focussing by the spectrometer.

(a) Stripping Reactions on a ⁴He Target

The ${}^4\text{He}({}^7\text{Li}, {}^6\text{Li}){}^5\text{He}$ and ${}^4\text{He}({}^7\text{Li}, {}^6\text{He}){}^5\text{Li}$ reactions were studied using beams of 50 MeV ${}^7\text{Li}$ ions, obtained from the ANU 14UD pelletron accelerator. The ${}^4\text{He}$ target consisted of a small gas cell (Hotchkis 1984) filled to a pressure of 100 Torr (≈ 13.3 kPa). The beam entered through a $560 \mu\text{g cm}^{-2}$ Ni window and was stopped inside the cell. Internal collimators were arranged so that only the central 1.4 cm of the gas (subtending 0.2°) was viewed by the spectrometer entrance slit. Reaction products emerging at 6° to the beam direction left the cell through a $490 \mu\text{g cm}^{-2}$ mylar window and were analysed in the spectrometer. The detector was operated in a transmission mode, and signals recording the position, angle and rate of energy loss were obtained for each event. These allowed clear identification of particle species. The resulting position spectra for the ${}^4\text{He}({}^7\text{Li}, {}^6\text{Li}){}^5\text{He}$ and ${}^4\text{He}({}^7\text{Li}, {}^6\text{He}){}^5\text{Li}$ reactions are shown in Figs 1*a* and 2*a* respectively.

During the ${}^4\text{He}({}^7\text{Li}, {}^6\text{Li}){}^5\text{He}$ study, the ${}^4\text{He}$ gas was replaced periodically by CO_2 in order to provide sharp peaks in the focal plane spectra from reactions on the ${}^{16}\text{O}$. This allowed any shifts in the position signal to be monitored and also facilitated the position calibration of the focal plane. The gas handling system was subsequently evacuated and flushed with ${}^4\text{He}$ before the cell was refilled. Despite this precaution, small peaks from reactions on ${}^{16}\text{O}$ were evident in the final ${}^5\text{He}$ spectrum. One of these contaminant peaks lies beneath the ${}^5\text{He}$ lineshape, but was estimated to contain only 35 counts and hence to have a negligible effect on the spectrum.

Table 3. Uncertainties in calibrations

<i>(a) ${}^4\text{He}({}^7\text{Li}, {}^6\text{Li}){}^5\text{He}$ and ${}^4\text{He}({}^7\text{Li}, {}^6\text{He}){}^5\text{Li}$</i>						
Source	Uncertainty (keV)					
	${}^5\text{He}$	${}^5\text{Li}$				
Uncertainty in calibration procedure	± 6	± 8				
Uncertainty of $\pm 0.15^\circ$ in angle ^A	± 24	± 20				
Uncertainties in energy loss of ejectiles	± 9	± 15				
Uncertainty of ± 50 keV in beam energy	± 3	± 8				
Uncertainties in masses of other nuclei	± 1	± 1				
Shift in centroids between data from ${}^4\text{He}$ and CO_2 gas	± 2	—				
Total r.m.s. uncertainty ^B	± 27	± 28				

<i>(b) ${}^6\text{Li}({}^{12}\text{C}, {}^{13}\text{N}){}^5\text{He}$ and ${}^6\text{Li}({}^{13}\text{C}, {}^{14}\text{C}){}^5\text{Li}$</i>						
Source	Uncertainty (keV)					
	${}^5\text{He}$			${}^5\text{Li}$		
	3.62°	4.58°	5.12°	3.46°	4.61°	5.20°
Scatter of calibration points about fit ^C	± 20	± 25	± 17	± 18	± 14	± 20
Uncertainty of ± 50 keV in beam energy	± 7	± 7	± 5	± 8	± 4	± 7
Uncertainty of $\pm 0.03^\circ$ in angle ^D	± 7	± 8	± 12	± 3	± 8	± 8
Uncertainty of $\pm 40\%$ in target thickness	± 12	± 2	± 2	± 4	± 8	± 6
Uncertainties in masses of other nuclei	± 1	± 1	± 1	± 1	± 1	± 1
Total r.m.s. uncertainty ^B	± 25	± 27	± 21	± 20	± 18	± 23

^A Taken as the r.m.s. deviation of lab angles from their nominal values for pickup reactions.

^B The dominant contribution is an r.m.s. value, therefore the total uncertainty is approximately an r.m.s. value.

^C r.m.s. value.

^D Maximum uncertainty in lab angle determined from kinematic shifts as described in text.

The $^{16}\text{O}(^7\text{Li}, ^6\text{Li})^{17}\text{O}_{\text{g.s.}}$ peak in the ^5He spectrum was exploited to obtain an absolute calibration of the position spectrum. This peak occurred at a distance of 54 cm along the detector, whereas the ^5He data extended from 29 to 42 cm. The interval between 42 and 55 cm was calibrated using ($^7\text{Li}, ^6\text{Li}$) reaction peaks observed with CO_2 in the gas cell. At the completion of the ^5He data acquisition the magnetic field was increased by 9% and a second spectrum obtained with CO_2 in the gas cell. This gave peaks from 27 to 45 cm, completing the calibration. The total uncertainty in the final calibration was ± 27 keV and was dominated by the uncertainty in the reaction angle. This uncertainty, $\pm 0.15^\circ$, was estimated using the results of Section 2*b*. All of the individual contributions to the calibration uncertainty are included in Table 3*a*.

In the case of the $^4\text{He}(^7\text{Li}, ^6\text{He})^5\text{Li}$ study, the ^7Li peak corresponding to elastic scattering from ^4He was detected at the low-rigidity end of the focal plane and provided a continuous monitor of the position signal stability. Data were also collected with the target gas replaced by CO_2 for calibration purposes. Two independent determinations of the absolute value of the magnetic field were provided by the $^{12}\text{C}(^7\text{Li}, ^6\text{He})^{13}\text{N } \frac{5}{2}^+$, 3.547 MeV peak at 49 cm* and the $^4\text{He}(^7\text{Li}, ^4\text{He})^7\text{Li}$ peak at 39 cm; the resulting calibrations differed by only 2 keV. A dispersion calibration extending from 27 to 50 cm, spanning the region of the ^5Li data and both absolute calibration points, was obtained from scattering and single-nucleon transfer reactions at a single magnetic field. The total uncertainty in the calibration was ± 28 keV, the largest contribution again being that due to the uncertainty in the reaction angle (Table 3*a*).

(*b*) Pickup Reactions from a ^6Li Target

The $^6\text{Li}(^{12}\text{C}, ^{13}\text{N})^5\text{He}$ and $^6\text{Li}(^{13}\text{C}, ^{14}\text{C})^5\text{Li}$ reactions were studied using beams of 90 MeV ^{12}C and ^{13}C ions, incident on ^6LiF targets (Table 1). Measurements at several reaction angles tested the sensitivity of the properties deduced for the mass-5 nuclei to details of the reaction kinematics. The gas pressure in the focal plane detector was chosen so that the ^{13}N and ^{14}C ejectiles stopped within the volume of the detector. Signals measuring the focal plane position, angle, rate of energy loss and total energy were recorded, and combinations of these signals provided clean identification of the various particle types. Data were also collected using a ^7LiF target to assist in the calibration of the focal plane and in estimating the intensities of some possible contaminant peaks. The position spectra for the reactions are shown in Figs 1*b*–1*d* and 2*b*–2*d* respectively.

The stability of the position signal was monitored throughout the experiment via $^{19}\text{F}(^{12}\text{C}, ^{13}\text{N})^{18}\text{O}$ peaks for the ^5He data and $^{19}\text{F}(^{13}\text{C}, ^{14}\text{C})^{18}\text{F}$ peaks for the ^5Li data. Shifts of up to three channels were observed and appropriate corrections were made in the analysis.

The composition of the targets was monitored at intervals throughout the experiment. During collection of the ($^{13}\text{C}, ^{14}\text{C}$) data the elastically scattered $^{13}\text{C}^{6+}$ ions were focussed at the low-rigidity end of the focal plane. An absorber which normally masked off this region of the detector was removed periodically to allow collection of an elastic scattering spectrum. During collection of the ($^{12}\text{C}, ^{13}\text{N}$) data, elastic scattering was investigated in a similar manner by periodically lowering the

* We assume that the unresolved $\frac{3}{2}^-$, 3.511 MeV state is not populated via stripping from a ^{12}C target.

accelerator's terminal voltage to transmit a $^{12}\text{C}^{5+}$ beam having the same rigidity as the 90 MeV $^{12}\text{C}^{6+}$ ions and removing the absorber in the low-rigidity region. The resolution of the elastic scattering peaks remained approximately constant for several hours (for typical beam currents of 450 nA) and then deteriorated abruptly. It could be restored by adjusting the position of the target in order to expose a new region to the beam. The ratio of lithium to fluorine in the target depended on the precise target position and also decreased under beam bombardment, these factors producing estimated uncertainties of $\pm 50\%$ in the reaction cross sections given in Table 2.

The calibrations used reaction peaks of known Q -value that occurred in the same region of the focal plane and were collected simultaneously with the mass-5 data in each case. This procedure minimised the errors introduced by uncertainties in reaction angle and target thickness. The linearity of the calibration over the 6 cm region of interest was established at each angle and spectrometer setting. This was accomplished by changing to a $^{12}\text{C}^{5+}$ beam, inserting a carbon target covered by a thin layer of gold and recording the position of the elastic scattering peak as the beam energy was incremented in 1 MeV steps.

The calibrations were sensitive to the values adopted for the reaction angles, but these angles could be determined precisely from the positions of adjacent peaks produced by the same reaction off target nuclei of different mass. For example, peaks from the $^{19}\text{F}(^{12}\text{C}, ^{11}\text{C})^{20}\text{F}$ reaction to the 0.0 and 0.656 MeV states and the $^6\text{Li}(^{12}\text{C}, ^{11}\text{C})^7\text{Li}_{\text{g.s.}}$ reaction, which are separated by less than 2 cm at the detector, were used. The angles determined from the kinematics in this manner are listed in Table 2. The individual contributions to the uncertainties in the calibrations are itemised in Table 3*b*. The largest contributions are from the scatter of the calibration data about the fitted function in each case. These may derive from errors in the relative stopping powers assumed for the different ejectiles and the effects of variations in the relative concentrations of lithium and fluorine within the target, as well as slight imperfections in the spectrometer and the focal plane detector.

3. Results and Analysis

(a) Lineshape Fitting using R -matrix Theory

The data shown in Figs 1 and 2 have been fitted to theoretical expressions derived from an R -matrix formalism as described in BW. Briefly, it was assumed that only $\frac{3}{2}^-$ and $\frac{1}{2}^-$ states were required for a description of the low-lying structure, and that for each J only two states need be considered. In BW, one of these was assumed to lie at very high excitation energy, taken to be 100 MeV, while the resonance energy E_{1J} of the lower state, the reduced width amplitudes $\gamma_{\lambda J}$ and the boundary condition parameter B_J were fitted. These quantities were derived as functions of channel radius a from fits to the p -wave phase shifts determined from $^4\text{He}+p$ and $^4\text{He}+n$ scattering. The upper levels were required in order to obtain good fits to the scattering data. Theoretical lineshapes for the $\frac{3}{2}^-$ and $\frac{1}{2}^-$ levels were generated using equation (11) of BW for the stripping reactions on the ^4He target, and using equation (12) of BW for the pickup reactions on the ^6Li target. The essential difference between the two is that both the lower and upper levels of a given J may be populated in the stripping reaction with feeding amplitudes $G_{\lambda J}^{1/2}$ proportional to $\gamma_{\lambda J}$, whereas there is no population of the upper levels in pickup because they have negligible parentage in the ground state of ^6Li .

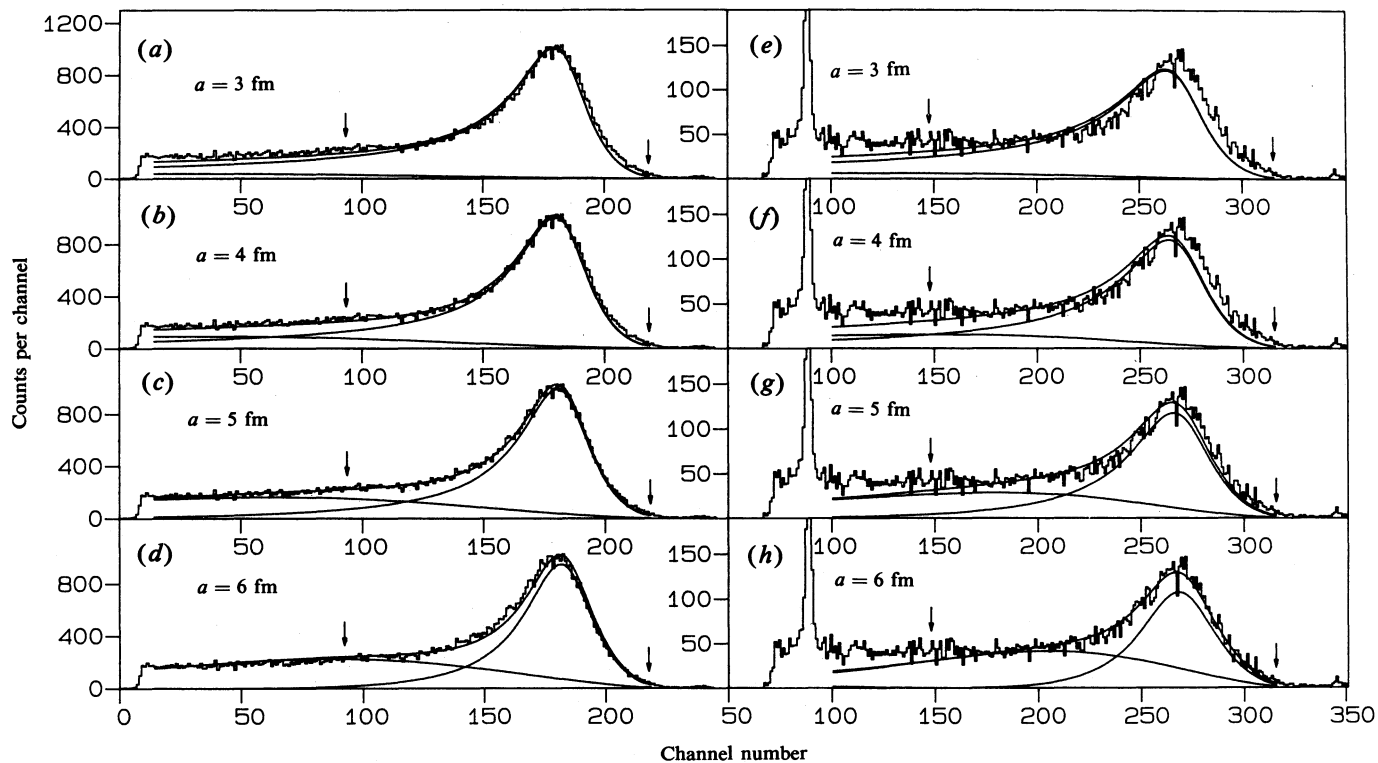


Fig. 3. Dependence of R -matrix fits to the stripping data on channel radius α : (a)–(d) for the ${}^4\text{He}({}^7\text{Li}, {}^6\text{Li}){}^5\text{He}$ reaction, and (e)–(h) for the ${}^4\text{He}({}^7\text{Li}, {}^6\text{He}){}^5\text{Li}$ reaction. Other details are as in Fig. 1.

After converting channel numbers in the position spectra to c.m. energies above the nucleon threshold, these theoretical lineshapes were fitted to the data. For a fixed value of the channel radius the only variable parameters were the ratio R of the $\frac{1}{2}^-$ strength to the $\frac{3}{2}^-$ strength and an overall normalisation. The fitted region in each spectrum was chosen for consistency to extend $2.5\Gamma_{1/2}$ to the left of the peak in each case, because this is approximately the smaller of the ranges over which the $p_{3/2}$ phase shifts were fitted in BW. The one exception to this was the ${}^6\text{Li}({}^{13}\text{C}, {}^{14}\text{C}){}^5\text{Li}$ data at 5.2° , in which a peak from the ${}^{19}\text{F}({}^{13}\text{C}, {}^{14}\text{C}){}^{18}\text{F}$ reaction limited the lower bound of the fitted region to $2\Gamma_{1/2}$ from the peak.

In BW it was noted that the sensitivity of the $\frac{3}{2}^-$ peak position to changes in channel radius is much greater for the stripping reactions than for pickup.* Approximate values of this sensitivity, defined as the change in peak position for a change in channel radius of 1 fm, are shown in Table 2. It is evident from a comparison of these sensitivities with the calibration uncertainties that a determination of a is possible only from the stripping data.

Table 4. Variation of quality of fits (χ^2) and R with a for ${}^4\text{He}({}^7\text{Li}, {}^6\text{Li}){}^5\text{He}$ and ${}^4\text{He}({}^7\text{Li}, {}^6\text{He}){}^5\text{Li}$

Reaction	Property	Calibration ^A	a (fm)				
			3	4	5	5.5	6
${}^4\text{He}({}^7\text{Li}, {}^6\text{Li}){}^5\text{He}$	χ^2 , ^B	$C-27$ keV	2.3	1.8	2.7	4.5	7.7
	χ^2	C	5.1	3.4	1.7	1.8	3.1
	χ^2	$C+27$ keV	10.9	8.1	4.1	2.6	1.9
	R , ^C	C	0.24	0.38	0.52	0.62	0.63
${}^4\text{He}({}^7\text{Li}, {}^6\text{He}){}^5\text{Li}$	χ^2	$C-28$ keV	3.3	2.5	1.6	1.3	1.2
	χ^2	C	3.9	3.1	2.0	1.5	1.2
	χ^2	$C+28$ keV	4.7	3.8	2.4	1.8	1.4
	R	C	0.20	0.35	0.53	0.58	0.71

^A C stands for central calibration for each reaction.

^B Values of chi-squared per degree of freedom. The errors on the number of counts in each channel were statistical only.

^C Ratio of $\frac{1}{2}^-$ and $\frac{3}{2}^-$ contributions to total lineshape.

Fits to the stripping reaction data were performed both for the best calibrations and for calibrations differing from these by energy shifts equal to the estimated r.m.s. uncertainties. Fig. 3 shows the fits obtained for the central calibrations for each integer value of a and Table 4 summarises the quality of the fits (parametrised as χ^2). The best fit to the ${}^4\text{He}({}^7\text{Li}, {}^6\text{Li}){}^5\text{He}$ data is obtained for $a \sim 5$ fm, whilst the ${}^4\text{He}({}^7\text{Li}, {}^6\text{He}){}^5\text{Li}$ data require $a \sim 6$ fm. Table 4 further illustrates the changes in quality as the calibrations are shifted, the best value of a for the ${}^5\text{He}$ data changing from 4 fm to slightly more than 6 fm. This would correspond to shifts of ± 1.5 channels in the theoretical lineshapes in Fig. 3. The ${}^5\text{Li}$ data favour a value of about 6 fm for all calibrations, although the variations in χ^2 are smaller than for ${}^5\text{He}$, due to the poorer statistical quality of the data. A value of 5.5 fm is adopted as the 'best' channel

* The values of energy and width given in Table 2 of BW for the $\frac{3}{2}^-$, ${}^4\text{He}+p$ resonance at $a = 3$ fm are incorrect, and should be replaced by 1.87 and 1.52 MeV in case a (stripping) and 1.90 and 1.66 MeV in case b (pickup).

radius, with an estimated uncertainty of ± 1 fm. Fits to the data for this channel radius are shown in Figs 1*a* and 2*a*.

For the pickup reactions ${}^6\text{Li}({}^{12}\text{C}, {}^{13}\text{N}){}^5\text{He}$ and ${}^6\text{Li}({}^{13}\text{C}, {}^{14}\text{C}){}^5\text{Li}$ fits were performed for a fixed channel radius of 5.5 fm only, for the reasons outlined above, and are shown in Figs 1*b–1d* and 2*b–2d*. The uncertainties in the calibrations correspond to shifts of approximately ± 1 channel in each case. The theoretical lineshapes agree with the data at all three angles for the ${}^6\text{Li}({}^{12}\text{C}, {}^{13}\text{N}){}^5\text{He}$ reaction and at the two smaller angles for the ${}^6\text{Li}({}^{13}\text{C}, {}^{14}\text{C}){}^5\text{Li}$ reaction. However, the positions of the theoretical and experimental maxima differ by three channels (78 keV) in the case of ${}^5\text{Li}$ at 5.2° (Fig. 2*d*), a discrepancy that is significantly larger than the uncertainty in the calibration. This difference is discussed in Section 3*b*.

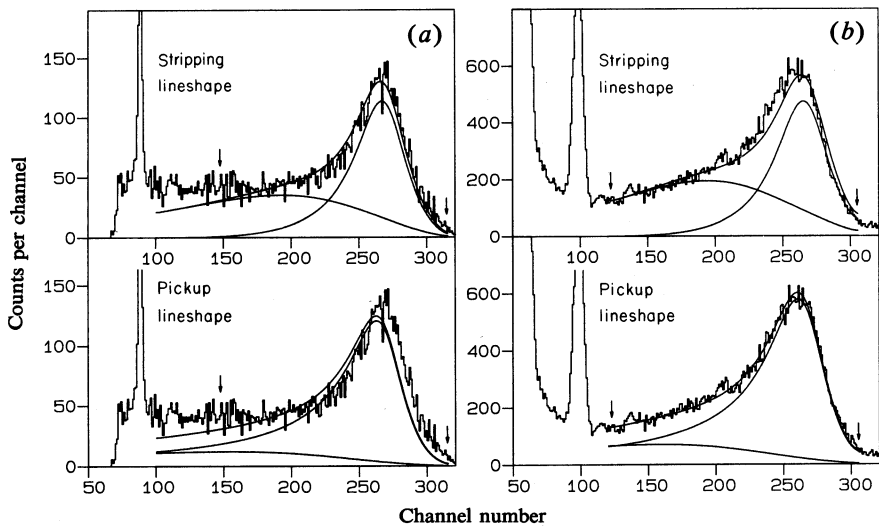


Fig. 4. Comparison of ${}^5\text{Li}$ *R*-matrix lineshapes for stripping and pickup, for $a = 5.5$ fm, (a) for the stripping reaction ${}^4\text{He}({}^7\text{Li}, {}^6\text{He}){}^5\text{Li}$ at 6° and (b) for the pickup reaction ${}^6\text{Li}({}^{13}\text{C}, {}^{14}\text{C}){}^5\text{Li}$ at 3.46° .

In order to test the sensitivity of the fits to the assumptions made about the feeding of the upper (100 MeV) $\frac{3}{2}^-$ and $\frac{1}{2}^-$ states, an attempt was made to fit the stripping reaction data with theoretical lineshapes derived assuming the upper levels were not fed (equation 12 of BW), which is equivalent to using the theoretical 'pickup' lineshape. The quality of the resulting fits was poor as shown in Fig. 4*a*. Specifically, for the ${}^4\text{He}({}^7\text{Li}, {}^6\text{He}){}^5\text{Li}$ reaction (Fig. 4*a*), the peak in the fit occurs four channels to the left of the data. This discrepancy is significantly larger than the uncertainty of ± 1.2 channels in the calibration, and changes by only 1.6 channels over the range of a values considered. For the ${}^4\text{He}({}^7\text{Li}, {}^6\text{Li}){}^5\text{He}$ reaction the 'pickup' lineshapes (not illustrated) are insensitive to the value of a and peak 1.5 channels to the left of the data, a discrepancy which is similar in size to the uncertainty in the calibration. It is concluded that feeding of the upper $\frac{3}{2}^-$ and $\frac{1}{2}^-$ levels is necessary for a proper description of the stripping reaction data, just as these levels were found to be necessary for an adequate description of the phase shift data.

In the same spirit, an attempt was made to fit the pickup data using the 'stripping' lineshapes, i.e. with feeding amplitudes of the $\frac{3}{2}^-$ and $\frac{1}{2}^-$ levels proportional to

their reduced width amplitudes (equation 11 of BW). This represents an unphysical situation in that it requires parentage of the very high-lying $\frac{3}{2}^-$ and $\frac{1}{2}^-$ levels in the ${}^6\text{Li}$ ground state. It was found that a good fit to the data could only be obtained for a small channel radius ($a \sim 3.5$ fm), which is inconsistent with the value of 5.5 fm obtained from the stripping reactions. The various fits are shown in Fig. 4b for the fixed value of $a = 5.5$ fm. The results demonstrate the dependence of the experimental spectra on the method of production of the mass-5 nuclei in direct reaction studies, and the importance of using appropriate values for the ratios of the feeding factors of the lower and upper levels in obtaining a consistent theoretical description of such data.

Table 5. Bound state and optical model potential parameters used in DWBA calculations

System	V_r^A (MeV)	r_r^B (fm)	a_r (fm)	V_{so}^A (MeV)	r_{so}^B (fm)	a_{so} (fm)	V_i^A (MeV)	r_i^B (fm)	a_i (fm)	$r_c^{B,C}$ (fm)
${}^5\text{He}+p$ ${}^5\text{He}+n$	Varied	1.583	0.45	10.0	1.10	0.65				1.83
${}^{12}\text{C}+p$ ${}^{13}\text{C}+n$	Varied	1.184	0.65	7.0	1.25	0.65				1.39
${}^{12}\text{C}+{}^6\text{Li}^D$	173.2	0.675	0.802				8.90	1.21	0.945	0.726
${}^{13}\text{C}+{}^6\text{Li}^D$	161.0	0.703	0.780				11.9	1.15	0.94	0.733

^A $V_k(r) = -V_k [1 + \exp(r - R_k)/a_k]^{-1}$ for $k = r, so, i$.

^B $R_k = r_k(A_t^{1/3} + A_p^{1/3})$ for optical potentials and $R_k = r_k A_t^{1/3}$ for bound states.

^C $V_c(r) = Z_p Z_t e^2 \{3 \cdot (r/R_c)^2\} / 2R_c$ for $r < R_c$ and $V_c(r) = Z_p Z_t e^2 / r$ for $r > R_c$.

^D Same optical model potentials used in entrance and exit channels.

(b) Comparison with DWBA Predictions for Pickup Reactions

The differential cross sections for the ${}^6\text{Li}({}^{12}\text{C}, {}^{13}\text{N}){}^5\text{He}$ and ${}^6\text{Li}({}^{13}\text{C}, {}^{14}\text{C}){}^5\text{Li}$ reactions at 90 MeV have been calculated in the distorted wave Born approximation (DWBA), using the exact finite-range code SATURN-MARS (Tamura and Low 1974). The bound state and optical model parameters are given in Table 5. The bound state potential for the target-residual nucleus system was chosen to reproduce the $6 \rightarrow 5$ separation energies and the r.m.s. charge radius of ${}^6\text{Li}$, which was taken as 2.57 fm (Bumiller *et al.* 1972). That for the projectile-ejectile system was chosen to give an r.m.s. charge radius of 2.47 fm for ${}^{12}\text{C}$, in agreement with the experimental value of Cardman *et al.* (1980). The optical potential employed for the ${}^6\text{Li}({}^{12}\text{C}, {}^{13}\text{N}){}^5\text{He}$ reaction was that used by Schumacher *et al.* (1973) for ${}^6\text{Li}$ scattering from ${}^{12}\text{C}$ at a c.m. energy of 24 MeV (compared with 30 MeV in the present experiment), and the potential employed for the ${}^6\text{Li}({}^{13}\text{C}, {}^{14}\text{C}){}^5\text{Li}$ reaction was that obtained by Zeller *et al.* (1979) for elastic scattering of ${}^6\text{Li}$ from ${}^{13}\text{C}$ at a c.m. energy of 27 MeV (compared with 28.5 MeV in the present experiment). The excitation energy of the $\frac{1}{2}^-$ state was taken as 3.0 MeV.

The predicted cross section to the $J^\pi = \frac{3}{2}^-$ or $\frac{1}{2}^-$ state in the mass-5 system is given by

$$\left(\frac{d\sigma}{d\Omega}\right)_J = (C^2 S)_H \left\{ \sum_{j=1/2, 3/2} (C^2 S)_L^j \left(\frac{d\sigma}{d\Omega}\right)_{SM}^j \right\}_J,$$

where $(C^2S)_H$ is the $(1p_{1/2})$ spectroscopic factor for the (heavy) projectile–ejectile system, $(C^2S)_L^j$ is the $(1p_j)$ spectroscopic factor for the (light) $6 \rightarrow 5$ system and $(d\sigma/d\Omega)_{SM}^j$ is the corresponding cross section obtained from SATURN-MARS.

Table 6. Spectroscopic factors S^j for the $6 \rightarrow 5$ system

J^π of mass-5 state	Orbital ($1p_j$)	CK ^A	vHG ^B	S^j B ^C	BW ^D	K ^E
$\frac{3}{2}^-$	$1p_{3/2}$	0.636	0.973	0.984	0.919	1.171
	$1p_{1/2}$	0.674	0.494	0.483	0.512	0.378
$\frac{1}{2}^-$	$1p_{3/2}$	0.674	0.494	0.483	0.512	0.378
	$1p_{1/2}$	0.016	0.038	0.050	0.057	0.075

A (6-16)2BME interaction of Cohen and Kurath (1967).

B van Hees and Glaudemans (1983, 1984).

C Barker (1966).

D 'Alternative interaction' of BW (1985).

E Kumar (1974).

Spectroscopic factors for the heavy system were taken from the (8-16)POT interaction of Cohen and Kurath (1967), which accurately reproduces the properties of nuclei in this mass region. Their interactions, however, are known to be less reliable for very light p-shell nuclei. Spectroscopic factors for the $6 \rightarrow 5$ system derived from various interactions are given in Table 6. The (6-16)2BME values of Cohen and Kurath (1967) differ significantly from those obtained from the interactions of Barker (1966), Kumar (1974) and BW, which were developed specifically to reproduce the properties of light nuclei, and from those obtained from the recent interaction of van Hees and Glaudemans (1983, 1984). The $6 \rightarrow 5$ spectroscopic factors from these four interactions are similar and those of Kumar (1974) are used in the ensuing discussion. The contributions from the two states do not interfere although their energies overlap, as implied by the formulae of Sharp *et al.* (1954), because the decay products of the mass-5 nuclei are not observed.

The calculated differential cross sections to the $\frac{3}{2}^-$ and $\frac{1}{2}^-$ states in ${}^5\text{He}$ and ${}^5\text{Li}$ are shown in Fig. 5. The angular distributions are similar over the range studied experimentally (from 11° to 18° in the c.m.). The resultant values of R for each reaction are therefore approximately the same at all three angles studied, but differ for the two reactions, which have very different Q -values. They are compared with the experimentally determined ratios in Table 7 and it is seen that the agreement is quite good, with the exception of the ${}^6\text{Li}({}^{13}\text{C}, {}^{14}\text{C}){}^5\text{Li}$ reaction at 5.2° . Values of R derived using the spectroscopic factors of Cohen and Kurath (Table 6) are larger than those given in Table 7 by 130%, 75% and 25% at 3.5° , 4.6° and 5.1° respectively, in marked disagreement with the experimental ratios. Values derived using the other spectroscopic factors in Table 6 are also between 5% and 54% larger, with the biggest discrepancies at the smallest angles.

The smallness of the empirical value of R for the ${}^6\text{Li}({}^{13}\text{C}, {}^{14}\text{C}){}^5\text{Li}$ reaction at 5.2° may be attributed to the inadequacy of the fit in this case. Inspection of the lineshapes (Fig. 2*d*) suggests that this might be caused by an error in the calibration and remedied by arbitrarily shifting the theoretical lineshape three channels to the right. This procedure, however, yielded a value of 0.11 for R , which is still less than half of the DWBA prediction, in contrast to the reasonable agreement between

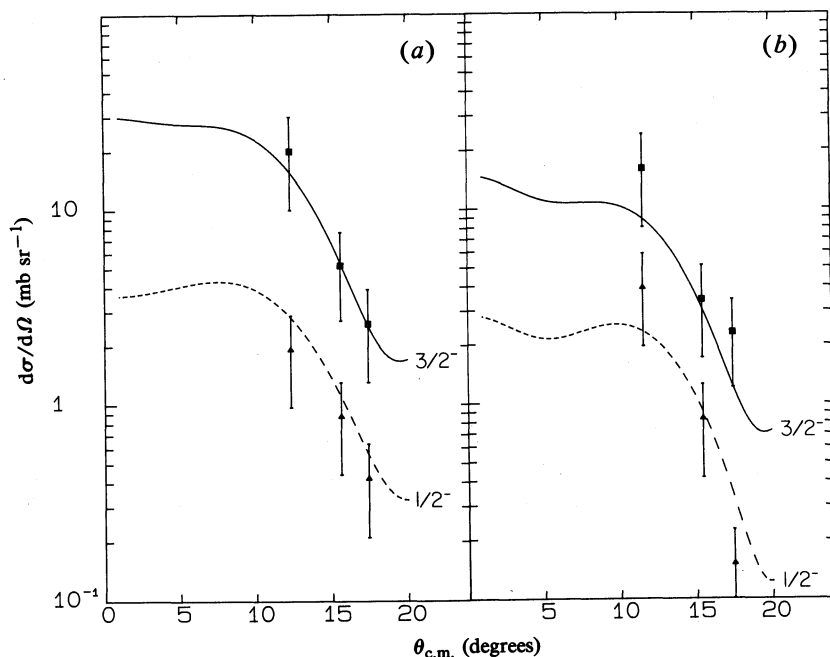


Fig. 5. Comparison of DWBA predictions for differential cross sections with experimental results for (a) the ${}^6\text{Li}({}^{12}\text{C}, {}^{13}\text{N}){}^5\text{He}$ reaction to the $\frac{3}{2}^-$ state (squares) and $\frac{1}{2}^-$ state (triangles) and (b) the ${}^6\text{Li}({}^{13}\text{C}, {}^{14}\text{C}){}^5\text{Li}$ reaction to the $\frac{3}{2}^-$ state (squares) and $\frac{1}{2}^-$ state (triangles).

Table 7. Ratio R of the $\frac{1}{2}^-$ strength to the $\frac{3}{2}^-$ strength for pickup reactions

Reaction	Quantity	Value		
${}^6\text{Li}({}^{12}\text{C}, {}^{13}\text{N}){}^5\text{He}$	θ_{lab}	3.62°	4.58°	5.12°
	$\theta_{\text{c.m.}}$	12.3°	15.6°	17.4°
	$R(\text{Fit})$	0.10	0.17	0.16
	$R(\text{DWBA})$	0.18	0.21	0.22
${}^6\text{Li}({}^{13}\text{C}, {}^{14}\text{C}){}^5\text{Li}$	θ_{lab}	3.46°	4.61°	5.20°
	$\theta_{\text{c.m.}}$	11.6°	15.5°	17.5°
	$R(\text{Fit})$	0.24	0.24	0.06 ^A
	$R(\text{DWBA})$	0.26	0.29	0.27

^A $R = 0.11$ when the theoretical lineshape is shifted artificially to fit data, which may contain significant contributions from other decay modes as described in Section 3b.

the DWBA and empirical values at the other two angles. The failure to fit the data at 5.2° is therefore unlikely to be due to a simple calibration error. The observed lineshape may be distorted by significant contributions from ${}^{14}\text{C}$ ions produced in processes such as ${}^{13}\text{C} + {}^6\text{Li} \rightarrow {}^{15}\text{N}^* + {}^4\text{He}$ followed by proton decay of the excited state of ${}^{15}\text{N}$, and in compound nuclear processes. The angular distributions of the ${}^{14}\text{C}$ nuclei originating in these alternative processes are expected to be approximately isotropic and therefore relatively more important at this largest angle, because the direct reaction cross section peaks at forward angles (Table 2).

The preceding analysis assumes that the $\frac{3}{2}^-$ and $\frac{1}{2}^-$ states are narrow, whereas they are actually broad and several factors change appreciably across their widths. These are: firstly, the geometrical conversion factor between laboratory and c.m. solid angle, which changes by approximately 2.5% per MeV; secondly, the conversion between laboratory and c.m. angle, which changes by approximately 1.3% per MeV; and thirdly, the DWBA cross sections for each state, which change by up to 16% per MeV. In a comparison between data and DWBA predictions the second and third effects are most easily treated together because the calculated cross sections are functions of angle and excitation energy. All three effects were examined in detail for each reaction at the smallest angle. It was found that fits of similar quality to those shown in Figs 1*b* and 2*b* were obtained, with the net effect being somewhat larger values of R , provided that the fitting region was restricted to an energy range of $2.5\Gamma_{1/2}$ from the peak energy, as in the analysis described above.

The experimental values of the c.m. cross sections for both reactions to the $\frac{3}{2}^-$ states are in good agreement with the DWBA predictions as illustrated in Fig. 5. The uncertainties in the absolute magnitudes of the DWBA cross sections to the $\frac{3}{2}^-$ states are estimated to be $\pm 50\%$, including contributions from uncertainties in the bound state and optical model potentials, the approximations inherent in the integration method employed in SATURN-MARS and the differences between spectroscopic factors from different interactions. The empirical $\frac{1}{2}^-$ cross sections shown in Fig. 5 were derived from the observed $\frac{3}{2}^-$ cross sections and the values of R determined by fitting the theoretical lineshapes to the data (Table 7). These also show reasonable agreement with the DWBA predictions although the differences between spectroscopic factors from different interactions are larger for this state.

DWBA calculations were not performed for the ${}^4\text{He}({}^7\text{Li}, {}^6\text{Li}){}^5\text{He}$ and ${}^4\text{He}({}^7\text{Li}, {}^6\text{He}){}^5\text{Li}$ stripping reactions, because of the difficulties associated with obtaining an adequate description of the unbound final states. An estimate of R which neglects any angle dependence may be obtained from equation (10) of BW. For the stripping cases, the J -dependence of the feeding factors and reduced widths cancel, giving a ratio of 0.5 from the $(2J+1)$ statistical factors alone. These are comparable with the empirical values of R , shown in Table 4.

4. Discussion

The conclusion from the preceding data analysis was that a consistent description of all the data was obtained for a channel radius of 5.5 fm.

(a) Results for $a = 5.5$ fm

The parameter values from which the theoretical lineshapes for this channel radius were generated are shown in Table 8. They were derived in the same manner as employed in BW for other channel radii. The uncertainties in these values due to the uncertainties in the phase shifts from which they were derived are very small, being of the same order as those given by Bond and Firk (1977) for the ${}^5\text{He}$ case (e.g. ± 0.3 keV for the $\frac{3}{2}^-$ resonance energy).* These uncertainties are henceforth

* The uncertainties given in Table VIII of Dodder *et al.* (1977) are not directly relevant, because their choice of boundary condition parameter, $B_J = 0$, is different from that given in equation (6) of BW, which is also used by Bond and Firk (1977).

Table 8. *R*-matrix parameters for $a = 5.5$ fm

Nucleus	J^π	E_{1J} (MeV)	γ_{1J} (MeV ^{1/2})	γ_{2J} (MeV ^{1/2})	B_J
⁵ He	$\frac{3}{2}^-$	0.897	0.912	4.895	-0.4883
	$\frac{1}{2}^-$	3.290	1.226	4.324	-0.2069
⁵ Li	$\frac{3}{2}^-$	1.861	0.952	4.886	-0.428
	$\frac{1}{2}^-$	4.196	1.241	4.313	-0.218

Table 9. *R*-matrix values of the peak energy and FWHM of the $\frac{3}{2}^-$ and $\frac{1}{2}^-$ levels for $a = 5.5$ fm

Method of production	$E_{\max}(\frac{3}{2}^-)$ (MeV \pm keV)		$\Gamma_{1/2}(\frac{3}{2}^-)$ (MeV \pm keV)		$E_{x,\max}(\frac{1}{2}^-)$ (MeV)		$\Gamma_{1/2}(\frac{1}{2}^-)$ (MeV)	
	⁵ He	⁵ Li	⁵ He	⁵ Li	⁵ He	⁵ Li	⁵ He	⁵ Li
Stripping	0.838 \pm 18	1.76 \pm 60	0.645 \pm 46	1.18 \pm 130	1.94 \pm 0.46	1.87 \pm 0.56	3.6 \pm 1.2	4.1 \pm 2.5
Pickup	0.869 \pm 3	1.86 \pm 10	0.723 \pm 19	1.44 \pm 80	2.58 \pm 0.40	2.68 \pm 0.50	5.3 \pm 2.3	6.1 \pm 2.8
Compilation ^A	0.89 \pm 50	1.96 \pm 50	0.60 \pm 20	\approx 1.5	4 \pm 1	5-10	4 \pm 1	5 \pm 2

^A Value adopted in compilation (Ajzenberg-Selove 1984).

neglected in comparison with the effects of changing the channel radius from its best value by ± 1 fm, the uncertainty adopted above.

The parameter values of Table 8 have been used to deduce the peak energies and widths of the $\frac{3}{2}^-$ ground states and $\frac{1}{2}^-$ first excited states of ${}^5\text{He}$ and ${}^5\text{Li}$ produced via stripping and pickup reactions and these are given in Table 9. The errors quoted in each case reflect the uncertainty of ± 1 fm in the channel radius. Because the uncertainty in the channel radius was determined mainly by fitting the properties of the $\frac{3}{2}^-$ states observed via stripping reactions, it follows that in these two cases the uncertainties given in Table 9 are comparable with those in the calibration of the data (Table 2). Individual fits to the data could not yield such precise information on the properties of the $\frac{3}{2}^-$ states in the case of the pickup reactions or of the $\frac{1}{2}^-$ states; the precision given in Table 9 is based on the requirement that the properties of all the low-lying states be given by parameters corresponding to a channel radius of 5.5 ± 1.0 fm.

(b) Discussion of Earlier Work

As discussed in Section 3, the maximum energies of the peaks observed in direct reaction studies in which the resonances are formed by stripping reactions are expected to be different from those observed when they are formed by pickup reactions, because of the different relative feeding amplitudes to the background levels in the two cases. The $\frac{3}{2}^-$ and $\frac{1}{2}^-$ states of ${}^5\text{He}$ and ${}^5\text{Li}$ have been observed via a variety of reactions in earlier work, corresponding to different relative feeding amplitudes to the lower and upper levels. In all cases, however, the analyses employed a one-level approximation, for which the parameters E_{max} and $\Gamma_{1/2}$ are independent of the reaction mechanism. Despite these problems, the reaction values and the ${}^4\text{He} + \text{nucleon}$ scattering results were averaged in a recent compilation (Ajzenberg-Selove 1984) and the averages are included in Table 9. These cannot be compared directly with our results because of the different experimental and analytical methods employed, but large discrepancies between the range of our values and the earlier averages are worthy of investigation.

The $\frac{3}{2}^-$ ground states. The energy of the $\frac{3}{2}^-$ state of ${}^5\text{Li}$, averaged from the earlier work, lies outside the range of our stripping and pickup results. The experiments from which the former is derived were performed before 1960 and all except one gave values ranging from 1.65 to 1.99 MeV, with errors of between 100 and 200 keV. The exceptional value of 2.03 ± 0.04 MeV, given by Rybka and Katz (1958), however, significantly affects the adopted value because of its comparatively small error. Briefly, their work comprised a study of (γ, n) reactions from a natural lithium target irradiated by bremsstrahlung, the maximum energy of which was varied in small steps. They interpreted small changes in the slope of the neutron yield curve as the thresholds of different reactions, deducing the above value for the ${}^5\text{Li}$ ground state energy. The corresponding change in slope is not, however, apparent in the published yield curve, even allowing for the large level width.

In addition to the data considered in the compilation, an experimental study of the properties of ${}^5\text{Li}$ has been published recently by Yasnogorodskii (1986). He studied the ${}^3\text{He}(\alpha, d){}^5\text{Li}$ reaction at an incident energy of 26.5 MeV, estimating and subtracting the three-body breakup contribution from the deuteron spectrum and fitting two Gaussian or Lorentzian peaks to the remainder. From these, he derived the properties of the $\frac{3}{2}^-$ and $\frac{1}{2}^-$ states, obtaining an energy of 1.93 ± 0.21 MeV and width of 1.9 ± 0.25 MeV for the $\frac{3}{2}^-$ state.

The $\frac{1}{2}^-$ excited states. The excitation energies of the $\frac{1}{2}^-$ states deduced in this work are significantly lower than the previously adopted values (Table 9) and the value of 5.0 ± 0.7 MeV obtained subsequently for ${}^5\text{Li}$ by Arena *et al.* (1984). The present results for ${}^5\text{Li}$, however, are similar to those obtained in two recent experimental studies. Cecil *et al.* (1985) observed γ -rays from the decay of the 16.66 MeV $\frac{3}{2}^+$ state, populated in the ${}^2\text{H}({}^3\text{He}, \gamma){}^5\text{Li}$ reaction. They fitted the spectrum with an exponentially decreasing background plus $\frac{1}{2}^-$ and $\frac{3}{2}^-$ states of either Gaussian or Lorentzian shape, with the $\frac{3}{2}^-$ energy fixed at its adopted value. They were able to obtain satisfactory fits only for $\frac{1}{2}^-$ energies in the range 2.5 to 3.5 MeV, giving their final result as 3.0 ± 1.0 MeV. Yasnogorodskii (1986) derived an excitation energy of 2.82 ± 0.35 MeV for the $\frac{1}{2}^-$ state and commented that the range of values obtained in different experiments demonstrates that the properties of this level depend strongly on the production channel.

(c) Implications for Low-lying Positive-parity States

The value of 5.5 ± 1.0 fm derived for the channel radius in the present work also implies excitation energies of $5.4_{-2.4}^{+5.6}$ MeV and $5.1_{-2.3}^{+5.3}$ MeV for the lowest $\frac{1}{2}^+$ states of ${}^5\text{He}$ and ${}^5\text{Li}$ respectively (BW). The possible existence of broad low-lying positive-parity states, predicted by recent shell-model calculations, formed the motivation for the work undertaken in BW. The shell-model interaction of van Hees and Glaudemans (1983, 1984) predicts a broad $\frac{1}{2}^+$ state at about 7.4 MeV excitation, and the alternative interaction chosen in BW specifically to fit the properties of light nuclei predicts a broad $\frac{1}{2}^+$ state at 6.4 MeV. These are in general agreement with the energies deduced in the present work.

The presence of these low-lying $\frac{1}{2}^+$ states in ${}^5\text{He}$ and ${}^5\text{Li}$ was not deduced from previous analyses of $s_{1/2}$ ${}^4\text{He} + \text{nucleon}$ scattering data. This was due to the values of approximately 3 fm employed for the channel radius. For this value of a the data required only small resonance contributions and hence high energies were obtained for the $\frac{1}{2}^+$ states [e.g. 28 MeV in ${}^5\text{Li}$ in the analysis of Dodder *et al.* (1977)]. It was shown in BW, however, that channel radii in the range 3 to 6 fm all gave satisfactory descriptions of the s, p and d wave phase shifts, and that the larger radii implied much lower energies for the positive-parity states (Table 1 of BW). Based on these results and the shell-model predictions, a value of approximately 5.1 fm was advanced as the appropriate channel radius for R -matrix analyses for the mass-5 system, in good agreement with the value of 5.5 ± 1.0 fm obtained in the present work.

Similarly, the results of the present work imply excitation energies of approximately 12 MeV for the lowest $\frac{3}{2}^+$ and $\frac{5}{2}^+$ states of ${}^5\text{He}$ and ${}^5\text{Li}$, in reasonable agreement with values of 13–15 MeV from the shell-model calculations of van Hees and Glaudemans (1983, 1984) and BW.

5. Summary and Conclusions

In an earlier paper (BW) it was shown that satisfactory fits to the ${}^4\text{He} + \text{nucleon}$ scattering data could be obtained in an R -matrix formalism for a range of values of the channel radius a , each value being associated with unique values of the other parameters ($E_{\lambda J}$, $\gamma_{\lambda J}$ and B_J). The parameter sets for different a give differing predictions for the peak energy and FWHM of the $\frac{3}{2}^-$ and $\frac{1}{2}^-$ lineshapes observed via direct reactions. Each set also gives predictions that depend on the method

of production of the mass-5 nuclei. This dependence arises because the high-lying background $\frac{3}{2}^-$ and $\frac{1}{2}^-$ levels are populated in stripping reactions from a ${}^4\text{He}$ target but not in pickup from a ${}^6\text{Li}$ target since they have negligible parentage amplitudes in the ${}^6\text{Li}$ ground state.

In the present work, data have been obtained for the stripping reactions ${}^4\text{He}({}^7\text{Li}, {}^6\text{Li}){}^5\text{He}$ and ${}^4\text{He}({}^7\text{Li}, {}^6\text{He}){}^5\text{Li}$ and the pickup reactions ${}^6\text{Li}({}^{12}\text{C}, {}^{13}\text{N}){}^5\text{He}$ and ${}^6\text{Li}({}^{13}\text{C}, {}^{14}\text{C}){}^5\text{Li}$, in regimes that favour a direct reaction mechanism. The data provide a clear demonstration of the dependence of the observed lineshapes on the method of production and are well described using lineshapes generated in the R -matrix formalism of BW. In the case of the stripping reactions, the sensitivity of the R -matrix predictions to the channel radius and the precision of the data are sufficient to permit the selection of the parameter set corresponding to a channel radius of 5.5 fm as that affording the best description of the mass-5 nuclei. The uncertainty in a is estimated to be ± 1 fm.

The R -matrix parameter set for $a = 5.5$ fm is given in Table 8. These parameters are well defined and are not dependent on the method of production of the mass-5 systems, in contrast to the more commonly quoted experimental values of energy and width, which are not uniquely defined in the case of broad, unbound states near the particle threshold. The parameter values may be used to derive the values that would be observed in a particular experiment for the properties of the lowest states of each spin and parity in ${}^5\text{He}$ and ${}^5\text{Li}$, and therefore, with appropriate values of the feeding amplitudes, provide a description of the mass-5 systems below the deuteron-breakup threshold. These parameter values have been used to deduce the peak energies and widths of the $\frac{3}{2}^-$ ground states and $\frac{1}{2}^-$ first-excited states given in Table 9, which differ for pickup and stripping reactions as explained above.

Finally, this choice of parameter values implies resonance energies of 5.4 and 5.1 MeV above the ground states for the lowest $\frac{1}{2}^+$ states in ${}^5\text{He}$ and ${}^5\text{Li}$ respectively. These states have widths large compared with their energies and therefore cannot be identified directly in reaction studies. A model-dependent test of these predictions is, however, provided by the shell-model calculations of van Hees and Glaudemans (1983, 1984) and BW, which respectively yield energies of approximately 7.4 and 6.4 MeV for these levels, in agreement with the present work.

References

- Ajzenberg-Selove, F. (1984). *Nucl. Phys. A* **413**, 1.
 Arena, N., Cavallaro, S., Figuera, A. S., D'Agostino, P., Fazio, C., Giardina, G., and Mezzanares, F. (1984). *Lett. Nuovo Cimento* **41**, 59.
 Barker, F. C. (1966). *Nucl. Phys.* **83**, 418.
 Barker, F. C., and Woods, C. L. (1985). *Aust. J. Phys.* **38**, 563.
 Bond, J. E., and Firk, F. W. K. (1977). *Nucl. Phys. A* **287**, 317.
 Bumiller, F. A., Buskirk, F. R., Dyer, J. N., and Monson, W. A. (1972). *Phys. Rev. C* **5**, 391.
 Cardman, L. S., Lightbody, J. W., Jr, Penner, S., Fivozinsky, S. P., Maruyama, X. K., Trower, W. P., and Williamson, S. E. (1980). *Phys. Lett. B* **91**, 203.
 Cecil, F. E., Cole, D. M., Philbin, R., Jarmie, N., and Brown, R. E. (1985). *Phys. Rev. C* **32**, 690.
 Cohen, S., and Kurath, D. (1967). *Nucl. Phys. A* **101**, 1.
 Dodder, D. C., Hale, G. M., Jarmie, N., Jett, J. H., Keaton, P. W., Nisley, R. A., and Witte, K. (1977). *Phys. Rev. C* **15**, 518.
 Hotchkis, M. A. C. (1984). Ph.D. Thesis, ANU (unpublished).

- Kumar, N. (1974). *Nucl. Phys. A* **225**, 221.
- Ophel, T. R., and Johnston, A. (1978). *Nucl. Instrum.* **157**, 461.
- Rybka, T. W., and Katz, L. (1958). *Phys. Rev.* **110**, 1123.
- Schumacher, P., Ueta, N., Duhm, H. H., Kubo, K.-I., and Klages, W. J. (1973). *Nucl. Phys. A* **212**, 573.
- Sharp, W. T., Kennedy, J. M., Sears, B. J., and Hoyle, M. G. (1954). Tables of coefficients for angular distribution analysis, CRT-556 AECL-97. Atomic Energy Commission of Canada, Chalk River, Ontario.
- Tamura, T., and Low, K. S. (1974). *Comput. Phys. Commun.* **8**, 349.
- van Hees, A. G. M., and Glaudemans, P. W. M. (1983). *Z. Phys. A* **314**, 323.
- van Hees, A. G. M., and Glaudemans, P. W. M. (1984). *Z. Phys. A* **315**, 223.
- Yasnogorodskii, A. M. (1986). *Sov. J. Nucl. Phys.* **43**, 178.
- Zeller, A. F., Kemper, K. W., Weisser, D. C., Ophel, T. R., Hebbard, D. F., and Johnston, A. (1979). *Nucl. Phys. A* **323**, 477.

Manuscript received 8 December 1987, accepted 17 February 1988